A Sectorized Beamspace Adaptive Diversity Combiner for Multipath Environments

Ta-Sung Lee, *Member, IEEE*, and Zong Si Lee

***Abstract*— The beam diversity technique is effective in combating multipath fading in wireless communications. In a beam diversity system, multiple receiving branches are formed with multiple antenna beams with distinctive patterns. These beams are synthesized in such a fashion that the fading phenomena observed at different branches are nearly uncorrelated. The disadvantage of such a system is the lack of adaptivity for cochannel interference (CCI) suppression. In this paper, an adaptive beam diversity combiner is proposed for sectorized signal reception. The diversity branches are formed with several adaptive beamformers whose response patterns encompass an angular sector in the field-of-view of the receiver. With a set of judiciously chosen weight vectors, effective diversity combining can be achieved inside the sector, and out-of-sector CCI can be suppressed via nulling. Simulation results confirm the efficacy of the proposed scheme.**

***Index Terms*—Adaptive antenna, beamforming, diversity combiner, sectorization.**

I. Introduction

IN WIRELESS communications, the channel is usually impaired by multipath fading. To achieve a reliable communication quality, some kind of diversity reception technique must be used [1]. In a diversity receiver, several branches are formed in such a fashion that the fading phenomena observed on the branch outputs are statistically uncorrelated. Popular diversity techniques include: space diversity, frequency diversity, time diversity, polarization diversity, and beam (pattern) diversity. Among these the space diversity technique is widely used due to its simple and economical implementation and that no extra frequency bands are required. The beam diversity technique can be regarded as a "beamspace" version of the space diversity technique in that the decorrelation of fading phenomena is performed using multiple beams pointed at different directions in space. Owing to the disparity of receiving patterns, the incoming multipath components add up in different ways resulting in noncoherent fading effects at different beams. Experimental results demonstrated that beam diversity is effective in decorrelating the branch signals [1]–[3].

The beam diversity receiver is suitable for sectorized signal reception. In sectorized signal reception, the entire field-of-view of the receiver is divided into several angular sectors,

Manuscript received March 15, 1998; revised August 20, 1998. This work was supported by the National Science Council of the Republic of China under Grant NSC 87-2213-E-009-038.

The authors are with the Department of Communication Engineering, National Chiao Tung University, Hsinchu, Taiwan, R.O.C.

Publisher Item Identifier S 0018-9545(99)05743-6.

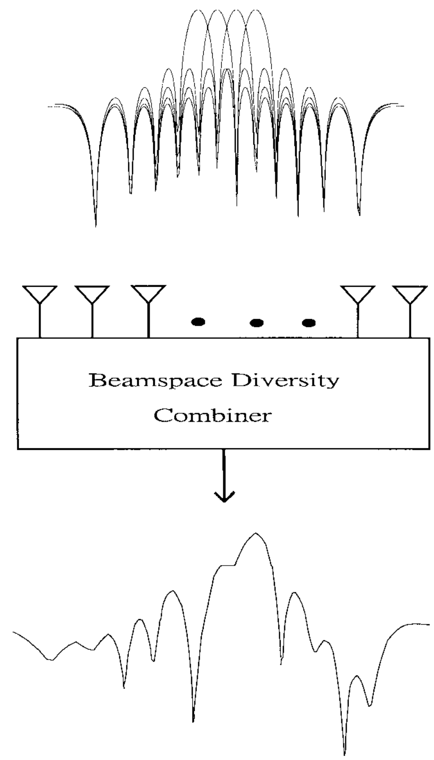

Fig. 1. Illustration of proposed diversity combing scheme.

with each sector responsible for a distinctive set of users. This provides a potential solution for increasing the capacity of the communication channel allocated to the system [4]. Incorporation of beam diversity in sectorized signal reception dictates the formation of a set of narrow beams encompassing the desired working sector. Cochannel interference (CCI) from outside the working sector will be suppressed through the sidelobes of the beams. This is illustrated in Fig. 1. The beam diversity receivers are nonadaptive in that the beam patterns associated with different branches are essentially fixed. A fixed beam diversity receiver lacks the flexibility of adapting in response to the environmental changes. For example, the fading effects due to a source observed at the receiver are different for different ranges and directions. Also, strong out-of-sector CCI will cause severe performance degradation. To achieve the optimum reception of source signals, the diversity receiver should be able to respond to both multipath scenario of signal and strong CCI. The adaptivity is twofold: both the formation of diversity beams and post-combining of these beams are executed adaptively.

In this paper, an adaptive beam diversity combiner is proposed for sectorized signal reception. The combiner is designed to meet two requirements. First, the diversity beams encompassing a prescribed angular sector is combined in such a fashion that the resulting signal-to-noise ratio (SNR) is maximized. Second, strong CCI from outside the sector should be suppressed in the sidelobe region of the combined beam. These can be accomplished by a two-stage procedure: performing adaptive nulling for each diversity beam first, then combine the adaptive beams with the maximum ratio criterion [5]. To avoid the signal cancellation phenomenon incurred with coherent multipaths or mismatch of steering vectors in adaptive nulling [6], a signal-blocking transformation is incorporated. The transformation is constructed so as to minimize the difference between the original and transformed array data subject to the constraint that the signals from inside the sector are effectively removed. The transformed data, which contain only the CCI and noise, are then used to construct a bank of linearly constrained minimum variance (LCMV) beamformers [7] for adaptive nulling. Finally, these LCMV beamformers are combined into a single beam in accordance with the maximum SNR criterion. The combined beam has the effect of "collecting" the multipath components in a constructive way. This is similar in principle to the RAKE receiver employed in code-division multiple access (CDMA) systems [8]. By cascading the two stages (nulling and combining), a single beamformer giving nearly the maximum signal-to-interference-plus-noise ratio (SINR) is obtained. This is again illustrated in Fig. 1. An alternative approach, termed optimum combining, was proposed as a minimum mean-square error receiver which achieves the maximum SINR using a single-stage procedure [9]. However, the optimum combiner requires a reference signal (training signal) for computing the weight vector, which may not be available in practice. Instead, the optimum combiner can be used in conjunction with the proposed combiner in that upon convergence, the proposed combiner can be switched into the optimum combiner working in the decision directed mode [10]. To evaluate the behavior of the proposed combiner, some performance issues are discussed, and numerical examples are given demonstrating the efficacy of the two-stage procedure in various environmental settings.

II. Array Data Model

Consider a narrowband multipath fading channel in which the field incident on the receiver due to the source is composed of a number of reflected waves with random gains and phases. The receive antenna is an array consisting of M elements. The multipath reflections are assumed to follow the local scattering model frequently used in urban-area wireless communications [5], [11]. The locally scattered multipaths associated with a source, as viewed from the receiver, are modeled as arriving from within some angular interval centered at the line-of-sight (LOS) angle. This is illustrated in Fig. 2, wherein $\Delta\theta$ is the angle spread, and θ_o is the line-of-sight (LOS) angle. In particular, for any θ_o, a set of random multipath angles are spread out over the interval $[\theta_o - \Delta\theta/2, \theta_o + \Delta\theta/2]$. In

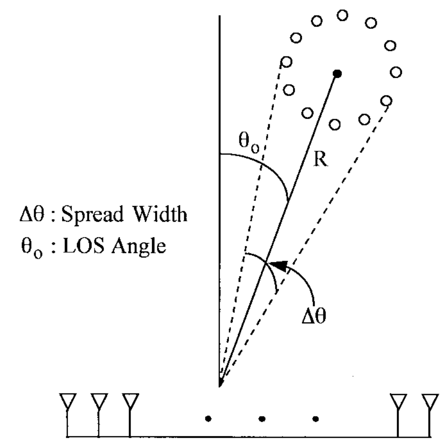

Fig. 2. Geometry of local scattering model.

general, the larger the range R between the source and receiver is, the smaller the angle spread $\Delta\theta$ will be, and *vice versa*. It is assumed that the delay spread [12] due to local scattering is small compared to the inverse bandwidth of the transmitted signal such that the flat fading assumption holds. Long-delay multipaths due to remote scatterers, which cause intersymbol interference (ISI), are treated as CCI.

With a source signal impinging on an array of M elements through a narrowband multipath fading channel, the baseband data received at the array at the kth sampling instant is given by the $M \times 1$ vector form

$$\begin{aligned} \boldsymbol{x}(k) &= \sum_{i=1}^{J} \alpha_i \boldsymbol{a}(\theta_i^p) s(k) + \boldsymbol{i}(k) + \boldsymbol{n}(k) \\ &= \boldsymbol{b} s(k) + \boldsymbol{i}(k) + \boldsymbol{n}(k) \end{aligned} \tag{1}$$

where J is the number of (locally scattered) multipaths, θ_i^p is the angle-of-arrival (AOA) of the ith path, and α_i is its associated complex gain. The α_i's are assumed independent and identically distributed complex Gaussian random variables. They are treated as constant over the processing period of interest due to the slow fading assumption. $\boldsymbol{a}(\theta)$ is the steering vector accounting for the gain/phase variation across the array, and

$$\boldsymbol{b} = \sum_{i=1}^{J} \alpha_i \boldsymbol{a}(\theta_i^p) \tag{2}$$

is the signal propagation vector due to the composition of J paths. Finally, $s(k)$, $\boldsymbol{i}(k)$, and $\boldsymbol{n}(k)$ are the source signal, CCI, and noise vectors, respectively, in baseband form. The components of $\boldsymbol{n}(k)$ are spatially white with the same power σ_n^2.

III. Development of Proposed Diversity Combiner

A beam diversity receiver results if we form N beams at the array, with each beam pointed at a distinctive look angle. Mathematically speaking, this represents transforming the array data vector $\boldsymbol{x}(k)$ into a set of scalar beamformer outputs

$$y_n(k) = \boldsymbol{w}_n^H \boldsymbol{x}(k), \qquad n = 1, \cdots, N \tag{3}$$

where $\boldsymbol{w}_n, n = 1, \cdots, N$, are the beamforming weight vectors, and H denotes the complex conjugate transpose. If the look angles are chosen such that the N beams cover a desired angular sector Θ in the field-of-view of the array, then a sectorized receiver results. By sectorization, it is meant that the signals from inside the sector are received through the main beams with a high gain, and CCI from outside the sector is suppressed through sidelobe cancellation. In other words, cochannel signals are discriminated via sector division.

A. Construction of Diversity Beamformers

To ensure an effective sidelobe cancellation in the presence of strong out-of-sector CCI, adaptive beamforming is performed for each of the N beams by choosing the weight vectors in accordance with the linearly constrained minimum variance (LCMV) criterion [7]

$$\begin{aligned}&\min_{\boldsymbol{w}_n} \quad E\{|y_n(k)|^2\} \equiv \boldsymbol{w}_n^H \boldsymbol{R}_{xx} \boldsymbol{w}_n \\ &\text{subject to: } \boldsymbol{w}_n^H \boldsymbol{a}(\theta_n^b) = 1, \qquad n = 1, \cdots, N \end{aligned} \tag{4}$$

where $\boldsymbol{R}_{xx} = E\{\boldsymbol{x}(k)\boldsymbol{x}^H(k)\}$ is the data-correlation matrix, and θ_n^b is the look angle of the nth beam. Invoking (1) and the spatial whiteness of the noise, we have

$$\boldsymbol{R}_{xx} = \sigma_s^2 \boldsymbol{b}\boldsymbol{b}^H + \boldsymbol{R}_{ii} + \sigma_n^2 \boldsymbol{I} \tag{5}$$

where $\sigma_s^2 = E\{|s(k)|^2\}$, $\boldsymbol{R}_{ii} = E\{\boldsymbol{i}(k)\boldsymbol{i}(k)^H\}$, and $\boldsymbol{I}$ is the identity matrix. The structure of (5) indicates that the expectation is taken for the source processes, treating $\boldsymbol{b}$ as deterministic. The solutions are well known to be given by

$$\boldsymbol{w}_n = \frac{1}{\boldsymbol{a}^H(\theta_n^b)\boldsymbol{R}_{xx}^{-1}\boldsymbol{a}(\theta_n^b)} \boldsymbol{R}_{xx}^{-1}\boldsymbol{a}(\theta_n^b), \qquad n = 1, \cdots, N. \tag{6}$$

A major problem of the direct implementation of LCMV beamforming is the phenomenon of desired signal cancellation [6] due to the statistical coherence among the multipath signals and the mismatch between the look angle steering vectors $\boldsymbol{a}(\theta_n^b)$'s and the composite steering vector $\boldsymbol{b}$. That is, each of the weight vectors in (6) will either combine the multipath components in a destructive manner (for a large $\Delta\theta$), or to put a null for these components (for a small $\Delta\theta$) in order to minimize the output power according to (4). An effective remedy to this is to block the signals before beamforming [6]. The rationale behind the success of signal blocking is that the beamformer will not attempt to suppress the signal if it cannot see the latter. The signal-blocking (SB) scheme (subtractive preprocessor) proposed in [6] is applicable only to the case of linear array and two coherent components. For the much more complicated scenario considered herein, a general solution is suggested which involves an $M \times M$ linear transformation $\boldsymbol{T}$ satisfying

$$\boldsymbol{T}\boldsymbol{a}(\theta_i^t) = \boldsymbol{0}, \qquad i = 1, \cdots, L \tag{7}$$

where θ_i^t, $i = 1, \cdots, L$, form a set of discrete angles well representative of the working sector Θ, and $\boldsymbol{0}$ is the zero vector. With a sufficiently large L, we have

$$\boldsymbol{T}\boldsymbol{x}(k) \approx \boldsymbol{T}\boldsymbol{i}(k) + \boldsymbol{T}\boldsymbol{n}(k). \tag{8}$$

We refer to $\boldsymbol{T}$ as the SB transformation. An LCMV beamformer working with the SB transformed data $\boldsymbol{T}\boldsymbol{x}(k)$ will not cancel the signal, but will instead put all its efforts in suppressing the transformed CCI $\boldsymbol{T}\boldsymbol{i}(k)$ and noise $\boldsymbol{T}\boldsymbol{n}(k)$. It is then easily seen that in order for the beamformers to work properly with the transformed data, the remaining degree of freedom in $\boldsymbol{T}$ should be exploited to minimize the error

$$E\{\|\boldsymbol{T}\boldsymbol{x}(k) - \boldsymbol{x}(k)\|^2\} \equiv \mathrm{tr}\{(\boldsymbol{T} - \boldsymbol{I})\boldsymbol{R}_{xx}(\boldsymbol{T} - \boldsymbol{I})^H\} \tag{9}$$

where $\|\cdot\|$ and $\mathrm{tr}\{\cdot\}$ denote the 2-norm and trace operator, respectively. Incorporation of the linear constraints of (7) in the minimization of (9) leads to the following constrained problem:

$$\begin{aligned}&\min_{\boldsymbol{T}} \quad \mathrm{tr}\{(\boldsymbol{T} - \boldsymbol{I})\boldsymbol{R}_{xx}(\boldsymbol{T} - \boldsymbol{I})^H\} \\ &\text{subject to: } \boldsymbol{T}\boldsymbol{A}_t = \mathbf{O}\end{aligned} \tag{10}$$

where $\boldsymbol{A}_t = [\boldsymbol{a}(\theta_1^t), \cdots, \boldsymbol{a}(\theta_L^t)]$ and $\mathbf{O}$ is the zero matrix. Some matrix calculus yields [13]

$$\boldsymbol{T} = \boldsymbol{I} - \boldsymbol{A}_t(\boldsymbol{A}_t^H \boldsymbol{R}_{xx}^{-1} \boldsymbol{A}_t)^{-1} \boldsymbol{A}_t^H \boldsymbol{R}_{xx}^{-1}. \tag{11}$$

According to (10), the SB transformed correlation matrix $\boldsymbol{T}\boldsymbol{R}_{xx}\boldsymbol{T}^H$ is the matrix closest to $\boldsymbol{R}_{xx}$ with the signals from inside Θ effectively removed. In fact, it is an estimate of the CCI-plus-noise correlation matrix given by

$$\boldsymbol{R}_{in} = \boldsymbol{R}_{ii} + \sigma_n^2 \boldsymbol{I}. \tag{12}$$

It follows that using $\boldsymbol{T}\boldsymbol{R}_{xx}\boldsymbol{T}^H$ in place of $\boldsymbol{R}_{xx}$ in (4)–(6) should give a set of beamformers which maximizes the output SINR at the look angles θ_n^b's without signal cancellation. However, since $\boldsymbol{T}$ is singular, we deliberately add a pseudonoise term to avoid inverting $\boldsymbol{T}\boldsymbol{R}_{xx}\boldsymbol{T}^H$. This leads to the pseudonoise injected SB transformed correlation matrix

$$\begin{aligned}\tilde{\boldsymbol{R}}_{xx} &= \boldsymbol{T}\boldsymbol{R}_{xx}\boldsymbol{T}^H + \eta \boldsymbol{I} \\ &= \boldsymbol{R}_{xx} + \eta \boldsymbol{I} - \boldsymbol{A}_t(\boldsymbol{A}_t^H \boldsymbol{R}_{xx}^{-1} \boldsymbol{A}_t)^{-1} \boldsymbol{A}_t^H\end{aligned} \tag{13}$$

where we have substituted (11). The pseudonoise also has the function of "masking" the residual desired signal not removed by $\boldsymbol{T}$, and can help to improve signal reception in Θ [14]. It should be chosen large enough to de-emphasize the desired signal, but not too large to distort the interference-plus-noise scenario. A suitable choice which proves to offer robustness against signal scenario variation is such that $\sigma_s^2 < \eta < M\sigma_s^2$. This means that the beamformers will only put efforts to eliminate CCI significantly stronger than the desired signal. Finally, the set of SB transformed LCMV weight vectors are obtained by replacing $\boldsymbol{R}_{xx}$ with $\tilde{\boldsymbol{R}}_{xx}$ in (6)

$$\tilde{\boldsymbol{w}}_n = \frac{1}{\boldsymbol{a}^H(\theta_n^b)\tilde{\boldsymbol{R}}_{xx}^{-1}\boldsymbol{a}(\theta_n^b)} \tilde{\boldsymbol{R}}_{xx}^{-1}\boldsymbol{a}(\theta_n^b), \qquad n = 1, \cdots, N. \tag{14}$$

B. The Maximum Ratio Combiner

The weight vectors $\tilde{\boldsymbol{w}}_n$'s produce N beams with diversity reception for the desired signal from Θ and adaptive cancellation for the CCI from outside Θ. These beams are then linearly combined into a single beam

$$\boldsymbol{w} = \sum_{n=1}^{N} g_n \tilde{\boldsymbol{w}}_n = \boldsymbol{W}\boldsymbol{g} \tag{15}$$

where $\boldsymbol{W} = [\tilde{\boldsymbol{w}}_1, \cdots, \tilde{\boldsymbol{w}}_N]$ and $\boldsymbol{g} = [g_1, \cdots, g_N]$ is the combining coefficient vector. To achieve the optimum performance, the vector $\boldsymbol{g}$ is determined in accordance with the maximum ratio combining (MRC) criterion [5]

$$\max_{\boldsymbol{g}} \frac{E\{|\boldsymbol{g}^H \boldsymbol{W}^H \boldsymbol{b} s(k)|^2\}}{E\{|\boldsymbol{g}^H \boldsymbol{W}^H \boldsymbol{n}(k)|^2\}}. \tag{16}$$

Unfortunately, the signal propagation vector $\boldsymbol{b}$ is not available in practice. A feasible alternative is to replace the combiner signal output power in the numerator of (16) by the combiner total output power $E\{|\boldsymbol{g}^H \boldsymbol{W}^H \boldsymbol{x}(k)|^2\}$. Note that with the out-of-sector CCI successfully suppressed by each diversity beamformer, the combiner total output power is approximately equal to the combiner signal-plus-noise output power, i.e.,

$$E\{|\boldsymbol{g}^H \boldsymbol{W}^H \boldsymbol{x}(k)|^2\} \approx E\{|\boldsymbol{g}^H \boldsymbol{W}^H \boldsymbol{b} s(k)|^2\} + E\{|\boldsymbol{g}^H \boldsymbol{W}^H \boldsymbol{n}(k)|^2\}. \tag{17}$$

Since maximizing the signal-plus-noise-to-noise ratio is effectively the same as maximizing the SNR, we can rewrite (16) as

$$\max_{\boldsymbol{g}} \frac{E\{|\boldsymbol{g}^H \boldsymbol{W}^H \boldsymbol{x}(k)|^2\}}{E\{|\boldsymbol{g}^H \boldsymbol{W}^H \boldsymbol{n}(k)|^2\}} \equiv \frac{\boldsymbol{g}^H \boldsymbol{W}^H \boldsymbol{R}_{xx} \boldsymbol{W} \boldsymbol{g}}{\sigma_n^2 \boldsymbol{g}^H \boldsymbol{W}^H \boldsymbol{W} \boldsymbol{g}} \tag{18}$$

whose solution is the dominant mode (eigenvector associated with maximum eigenvalue) of the eigenequation

$$\boldsymbol{W}^H \boldsymbol{R}_{xx} \boldsymbol{W} \boldsymbol{g} = \lambda \boldsymbol{W}^H \boldsymbol{W} \boldsymbol{g}. \tag{19}$$

An alternative expression for $\boldsymbol{w}$ can be obtained by substituting (5) in (19)

$$\boldsymbol{W}^H \boldsymbol{R}_{xx} \boldsymbol{W} \boldsymbol{g} \approx \sigma_s^2 \boldsymbol{W}^H \boldsymbol{b}\boldsymbol{b}^H \boldsymbol{W} \boldsymbol{g} + \sigma_n^2 \boldsymbol{W}^H \boldsymbol{W} \boldsymbol{g} = \lambda \boldsymbol{W}^H \boldsymbol{W} \boldsymbol{g} \tag{20}$$

where we have used the fact that the CCI is almost canceled by each of $\tilde{\boldsymbol{w}}_n$'s such that $\boldsymbol{W}^H \boldsymbol{R}_{ii} \boldsymbol{W} \approx \mathbf{O}$. It is easy to verify from (20) that the modified eigenequation has $N-1$ identical eigenvalues equal to σ_n^2 corresponding to the null space of $\boldsymbol{W}^H \boldsymbol{b}\boldsymbol{b}^H \boldsymbol{W}$, and the dominant mode corresponding to $\lambda > \sigma_n^2$ is given by

$$\boldsymbol{g} = \gamma (\boldsymbol{W}^H \boldsymbol{W})^{-1} \boldsymbol{W}^H \boldsymbol{b} \tag{21}$$

where $\gamma = (\lambda - \sigma_n^2)^{-1} \sigma_s^2 \boldsymbol{b}^H \boldsymbol{W} \boldsymbol{g}$ is a scalar. Finally, substituting (21) in (15) gives

$$\boldsymbol{w} = \gamma \boldsymbol{W} (\boldsymbol{W}^H \boldsymbol{W})^{-1} \boldsymbol{W}^H \boldsymbol{b}. \tag{22}$$

It is interesting to note that the last expression can be interpreted algebraically as the orthogonal projection of $\boldsymbol{b}$ onto the range space of $\boldsymbol{W}$. This makes sense since $\boldsymbol{b}$ is the optimum weight vector for signal reception under the quiescent (spatially white noise only) condition. On the other hand, the range space of $\boldsymbol{W}$ represents the subspace of CCI cancellation for the sector Θ. Projecting $\boldsymbol{b}$ orthogonally onto the range space of $\boldsymbol{W}$ is tantamount to finding a vector lying in the subspace of CCI cancellation which is closest to the optimum quiescent weight vector.

C. Algorithm Summary

In practice, the data correlation matrix is usually estimated by the sample average version

$$\hat{\boldsymbol{R}}_{xx} = \frac{1}{K} \sum_{k=1}^{K} \boldsymbol{x}(k) \boldsymbol{x}^H(k) \tag{23}$$

assuming that $\boldsymbol{x}(k)$ is stationary over the processing period K. Using the estimate, the proposed diversity combiner is summarized as follows.

1) Determine working sector Θ, constraint angles θ_i^t's, and look angles θ_n^b's.
2) Obtain $\hat{\boldsymbol{R}}_{xx}$ according to (23).
3) Compute $\tilde{\boldsymbol{R}}_{xx}$ according to (13), with $\boldsymbol{R}_{xx}$ replaced by $\hat{\boldsymbol{R}}_{xx}$.
4) Compute $\tilde{\boldsymbol{w}}_n$'s according to (14).
5) Compute $\boldsymbol{w}$ according to (15) and (19), with $\boldsymbol{R}_{xx}$ replaced by $\hat{\boldsymbol{R}}_{xx}$.

IV. Performance Issues

A. Tradeoff Between Diversity and CCI Cancellation

In an adaptive diversity combiner, the total degree of freedom for diversity reception and CCI cancellation is fixed. For example, if an M-element array is employed and N degrees of freedom are allocated to diversity reception, then the remaining $M - N - 1$ degrees of freedom are for CCI cancellation [9]. Although the adaptive beamformers in (14) appear to have access to the full degree of freedom of $M - 1$, using up the degrees of freedom for CCI will inevitably degrade the diversity performance. This is because that some degrees of freedom need be reserved for "shaping" the mainlobes of the N adaptive beamformers so that effective diversity can be achieved. For example, the degree of freedom for beamshaping for each of the $N = 4$ mainlobes in Fig. 1 is five, the number of sidelobe nulls inside the working sector.

On the other hand, the success of CCI cancellation depends largely on the success of retaining the CCI correlation matrix $\boldsymbol{R}_{ii}$ distortionlessly in $\tilde{\boldsymbol{R}}_{xx}$. This is possible only when a sufficiently large degree of freedom is reserved for minimizing the cost function in (10). By imposing L angle constraints in (10), the rank of $\boldsymbol{T}$ reduces from M to $M - L$, which represents a factor of L/M in reduction of its total degree of freedom. In general, a large L gives better "mainlobe performance" (reception of desired signal), and a small L gives better "sidelobe performance" (cancellation of CCI). A suitable choice for L which has been confirmed by simulations is such that $L \approx M/2$.

B. Sector Location and In-Sector CCI

To determine the working sector Θ, some kind of preliminary location method, such as spatial spectrum search, can be used to obtain a coarse estimate of the desired source direction (LOS angle). The estimate need not be accurate as required in conventional LCMV beamforming, but should lead to a sector encompassing the multipath arrivals. In this regard, the proposed combiner can be said to be "semiblind" in that effective beamforming can be achieved without the precise knowledge of signal direction. In a nonstationary environment in which the desired source moves with time, it is necessary to keep track of the source to update the sector position and $\boldsymbol{A}_t$. This can be done efficiently, for example, using the multibeam location technique [15]. In so doing, the outputs of the N diversity beamformers are used to determine the source direction via the amplitude comparison principle.

It is possible that there exist multiple cochannel signals in the working sector simultaneously. In this case, the diversity beamformers experience mainlobe CCI. The adaptive beamformers cannot cancel the mainlobe CCI since they have been removed by the SB transformation. A solution then would be to treat both the desired signal and CCI as target signals, and let the combiner extract these signals individually. It can be shown that if there are G $(G \leq N)$ in-sector signals, then the G most dominant eigenvectors of (19) will extract the G signals individually, as long as these signals are well separated in spatial angle [16]. That is, the combiner can "sort" through the in-sector signals by associating each one with an eigenvector. Some temporal scheme can be used to pick the right eigenvector for the desired signal. Note that the presence of multiple "large" eigenvalues in (19) can serve as an indicator of the existence of in-sector CCI.

C. Computational Complexity

The major computational load in the proposed algorithm involves the inversion of $\tilde{\boldsymbol{R}}_{xx}$ $(M \times M)$ in (14), which in turn requires the inversion of $\boldsymbol{R}_{xx}$ $(M \times M)$ and $\boldsymbol{A}_t^H \boldsymbol{R}_{xx}^{-1} \boldsymbol{A}_t$ $(L \times L)$ in (13). With the data-correlation matrix estimated by (23), inversion of these matrices can be performed via a fast algorithm such as that employed in recursive least square (RLS) filtering [10]. The eigendecomposition in (19) can be also performed efficiently since only the dominant mode is required.

Further simplification of the algorithm can be made if we invoke the matrix-inversion lemma [10] for inverting (13)

$$\begin{aligned}\tilde{\boldsymbol{R}}_{xx}^{-1} &= \boldsymbol{R}_\eta^{-1} - \boldsymbol{R}_\eta^{-1}\boldsymbol{A}_t(\boldsymbol{A}_t^H\boldsymbol{R}_\eta^{-1}\boldsymbol{A}_t - \boldsymbol{A}_t^H\boldsymbol{R}_{xx}^{-1}\boldsymbol{A}_t)^{-1}\boldsymbol{A}_t^H\boldsymbol{R}_\eta^{-1}\\ &\approx \boldsymbol{R}_\eta^{-1} + \frac{1}{\eta}\boldsymbol{R}_\eta^{-1}\boldsymbol{A}_t(\boldsymbol{A}_t^H\boldsymbol{R}_{xx}^{-2}\boldsymbol{A}_t)^{-1}\boldsymbol{A}_t^H\boldsymbol{R}_\eta^{-1}\\ &\approx \boldsymbol{R}_\eta^{-1} + \frac{1}{\eta}\boldsymbol{R}_\eta^{-1}\boldsymbol{A}_t(\boldsymbol{A}_t^H\boldsymbol{R}_\eta^{-2}\boldsymbol{A}_t)^{-1}\boldsymbol{A}_t^H\boldsymbol{R}_\eta^{-1} \qquad (24)\end{aligned}$$

where

$$\boldsymbol{R}_\eta = \boldsymbol{R}_{xx} + \eta\boldsymbol{I} \qquad (25)$$

and we have assumed that η is small compared to the diagonal entries of $\boldsymbol{R}_{xx}$ such that $\boldsymbol{R}_\eta^{-1} \approx \boldsymbol{R}_{xx}^{-1} + \eta\boldsymbol{R}_{xx}^{-2}$ and $\boldsymbol{R}_{xx}^{-2} \approx \boldsymbol{R}_\eta^{-2}$. The expression in (24) involves the inversion of $\boldsymbol{R}_\eta$ $(M \times M)$ and $\boldsymbol{A}_t^H\boldsymbol{R}_\eta^{-2}\boldsymbol{A}_t$ $(L \times L)$, which represents a saving of an $M \times M$ inversion compared to the original form.

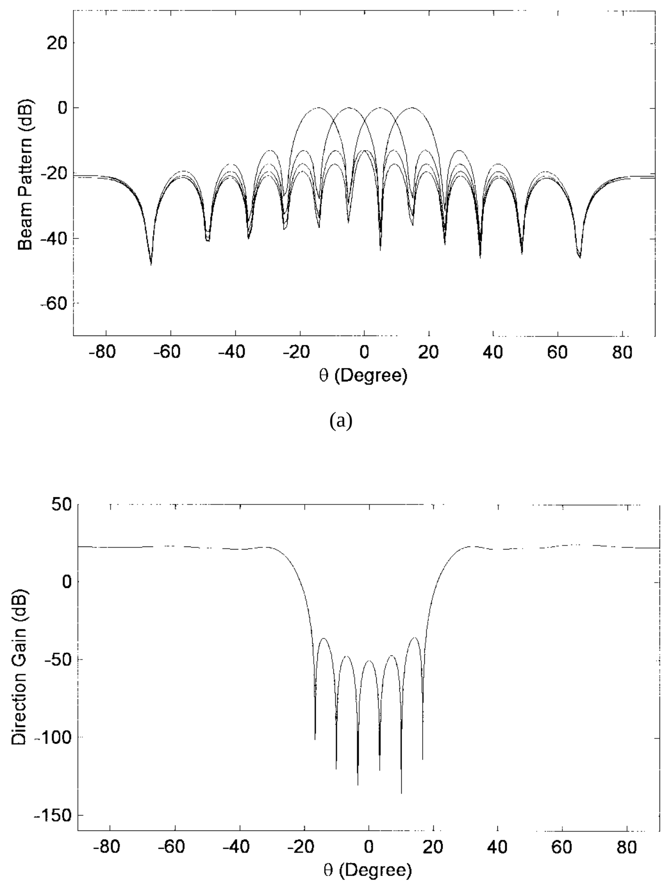

(a)

(b)

Fig. 3. (a) Patterns of nonadaptive beamformer bank. (b) Direction gain of SB transformation.

V. Computer Simulations

Computer simulations were conducted to demonstrate the performance of the proposed diversity combiner. The array employed was composed of $M = 12$ identical elements uniformly spaced by a half wavelength. The sector of interest was $\Theta = [-15°, 15°]$, and $N = 4$ beams were formed at look angles $\{-14.4°, -4.8°, 4.8°, 14.4°\}$, with adjacent beams equally spaced by a half 3-dB beamwidth of the array $(\approx 9.6°)$. The SB transformation $\boldsymbol{T}$ was set by choosing $L = 6$ constraint angles to be

$$\{-16.7°, -10.1°, -3.4°, 3.4°, 10.1°, 16.7°\}.$$

For reference, Fig. 3 shows the patterns of the nonadaptive beamformer bank and a typical example of the direction gain $T(\theta) = ||\boldsymbol{Ta}(\theta)||$ of the SB transformation. The desired signal impinged on the array via $J = 10$ paths, with incident angles uniformly distributed over the angular interval $[\theta_o - \Delta\theta/2, \theta_o + \Delta\theta/2]$. Two cochannel interferers, CCI-1 and CCI-2, impinged via ten paths with incident angles over $[45° - 5°, 45° + 5°]$ and $[\theta_1, \theta_1]$, respectively. The signal-to-interference ratio (SIR), measured for a single path, were -20 dB for CCI-1 and -10 dB for CCI-2. Note that CCI-2 was a point source with a variable incident angle. The pseudonoise power used in (13) was chosen to be $\eta = (M/2)\sigma_s^2 = 6$. The SNR, input

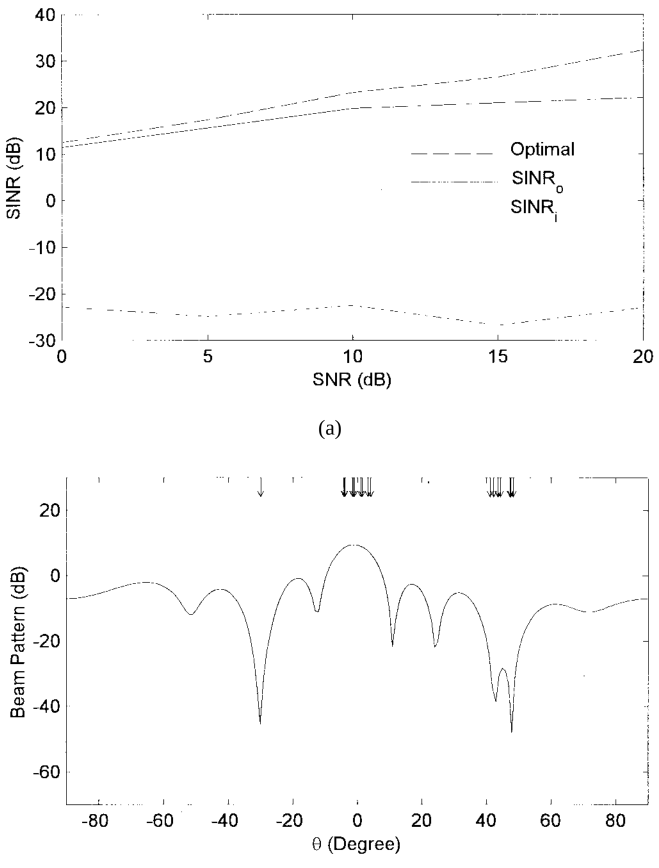

(a)

(b)

Fig. 4. Performance of proposed combiner as a function of input SNR. (a) Output SINR versus input SNR. (b) Pattern obtained with SNR = 10 dB.

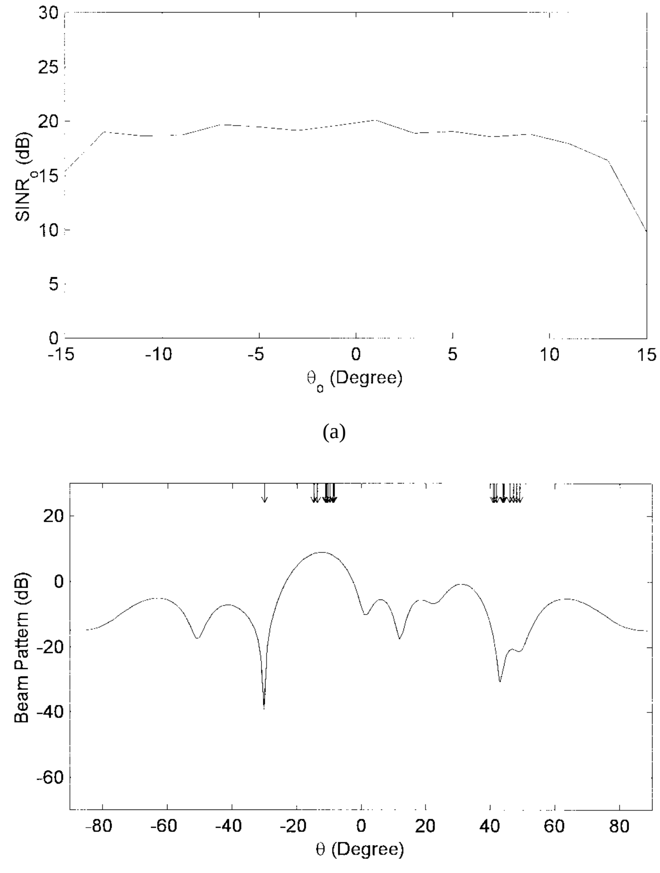

(a)

(b)

Fig. 5. Performance of proposed combiner as a function of LOS angle. (a) Output SINR versus θ_o. (b) Pattern obtained with $\theta_o = -10°$.

SINR, and output SINR (in decibels) were defined as

$$\text{SNR} = 10\log_{10}\frac{\sigma_s^2}{\sigma_n^2}$$
$$\text{SINR}_i = 10\log_{10}\frac{\sigma_s^2|\boldsymbol{b}(1)|^2}{\boldsymbol{R}_{ii}(1,1)+\sigma_n^2}$$
$$\text{SINR}_o = 10\log_{10}\frac{\sigma_s^2|\boldsymbol{w}^H\boldsymbol{b}|^2}{\boldsymbol{w}^H\boldsymbol{R}_{ii}\boldsymbol{w}+\sigma_n^2\boldsymbol{w}^H\boldsymbol{w}}$$

where $\boldsymbol{b}(1)$ and $\boldsymbol{R}_{ii}(1,1)$ denote the first and $(1,1)$th entry of $\boldsymbol{b}$ and $\boldsymbol{R}_{ii}$, respectively. In the above, SNR was defined for a single path, SINR$_i$ was defined for the composition of multipaths at the first element, and SINR$_o$ was defined at the combiner output. The difference between SINR$_i$ and SINR$_o$ measures the effect of using the combiner. In addition, we denote as SINR$_{\text{opt}}$ the output SINR obtained by the optimum combiner working with the weight vector $\boldsymbol{R}_{xx}^{-1}\boldsymbol{b}$ [7]. In each of the following simulation results, SINR statistics were obtained as an average from 100 independent trials, with each trial using a different set of unit variance complex gains α_i's and complex Gaussian random data sequence $\boldsymbol{x}(n)$ for constructing $\hat{\boldsymbol{R}}_{xx}$. Finally, the following "standard" parameters will be used throughout the section unless otherwise mentioned:

$$\text{SNR} = 10\text{ dB} \quad \theta_o = 0° \quad \Delta\theta = 10°$$
$$\theta_1 = -30° \quad K = 500.$$

The first simulation evaluates the output SINR performance of the proposed combiner as a function of SNR. The result in Fig. 4(a) shows that the combiner effectively collects the multipath components in a coherent way. In particular, the difference between SINR$_i$ and SINR$_o$ confirms that the two CCI's are successfully suppressed. However, the "saturation" of the SINR$_o$ curve at high SNR, as compared to SINR$_{\text{opt}}$ reveals that the combiner cannot cancel the CCI's completely. This is because that the interference vector is slightly distorted by the SB transformation such that the beamformer cannot put exact nulls for the CCI's. The combined pattern (associated with a selected trial) is shown in Fig. 4(b) for the case of SNR = 10 dB. It shows that the combiner produces a broad mainlobe for simultaneous reception of the desired multipath components, and nulls to block the CCI's.

The second simulation examines the effect of signal LOS angle θ_o. In this case, θ_o varied from $-15°$ to $15°$. Note that in the extreme cases of $\theta_o \approx \pm 15°$, the SB transformation is not able to remove some multipath components. This leads to a certain degradation in performance at both ends of the output SINR plot shown in Fig. 5(a). For a moderate deviation in θ_o, the combiner performs quite reliably, confirming that the desired signal can be received effectively over a large angular region in Θ. As an example, the combined pattern given in Fig. 5(b) for $\theta_o = -10°$ indicates that the combiner achieves

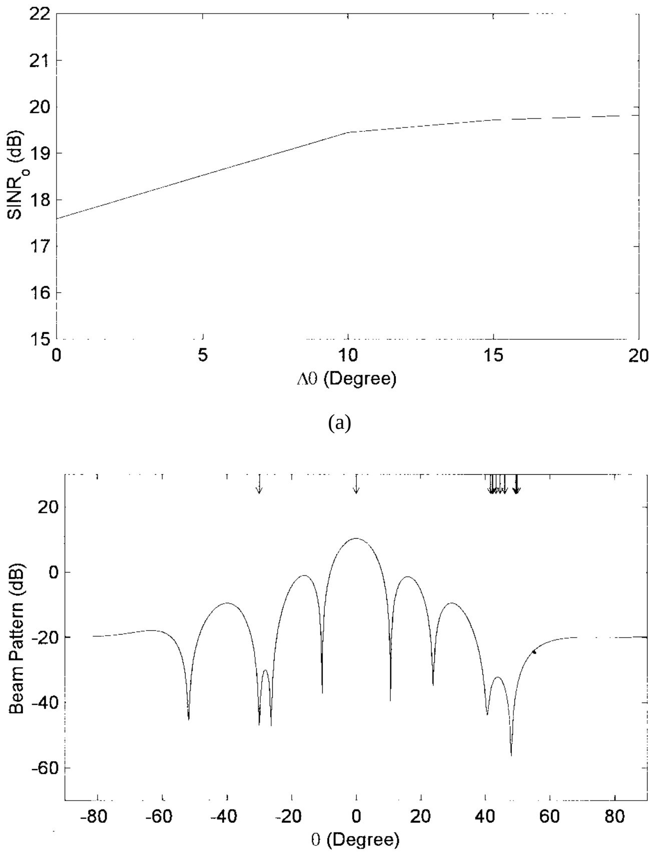

(a)

(b)

Fig. 6. Performance of proposed combiner as a function of angle spread. (a) Output SINR versus $\Delta\theta$. (b) Pattern obtained with $\Delta\theta = 0^\circ$.

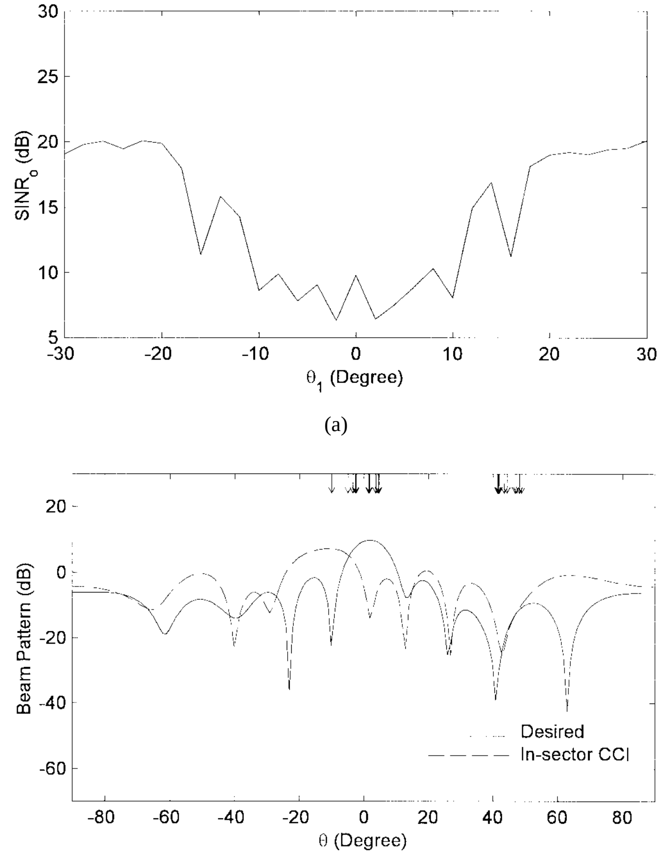

(a)

(b)

Fig. 7. Performance of proposed combiner in the presence of in-sector CCI. (a) Output SINR versus θ_1. (b) Pattern obtained with $\theta_1 = -10^\circ$.

this by "steering" its mainlobe to keep track of the desired signal.

The third simulation examines the effect of angle spread $\Delta\theta$ of the signal multipath distribution. In this case, $\Delta\theta$ varied from 0° to 20°. The result plotted in Fig. 6(a) shows that combining is performed better for a large $\Delta\theta$. This is consistent with the observation that a better diversity reception is achieved with a large multipath angle spread [17]. To see that the proposed combiner works for a point source, we show in Fig. 6(b) the combined pattern obtained with $\Delta\theta = 0^\circ$. Again, both the mainlobe and CCI nulls are synthesized as desired, indicating that the combiner behaves exactly like the conventional LCMV beamformer.

The fourth set of simulations evaluates the capability of the proposed combiner in combating in-sector CCI. In this case, the incident angle θ_1 of CCI-2 was varied from -30° to 30°. It was assumed that the correct eigenvector was always chosen for extracting the desired signal when the CCI was inside the working sector. The result plotted in Fig. 7(a) shows that an effective combining can be maintained in the presence of in-sector CCI, as long as θ_1 is not too close to the signal multipath region. To demonstrate the signal screening property of the eigen-based combiner, we give in Fig. 7(b) the patterns associated with the two dominant modes for $\theta_1 = -10^\circ$. Clearly, the combiner extracts the two signals individually by forming two beams pointed at the respective source directions.

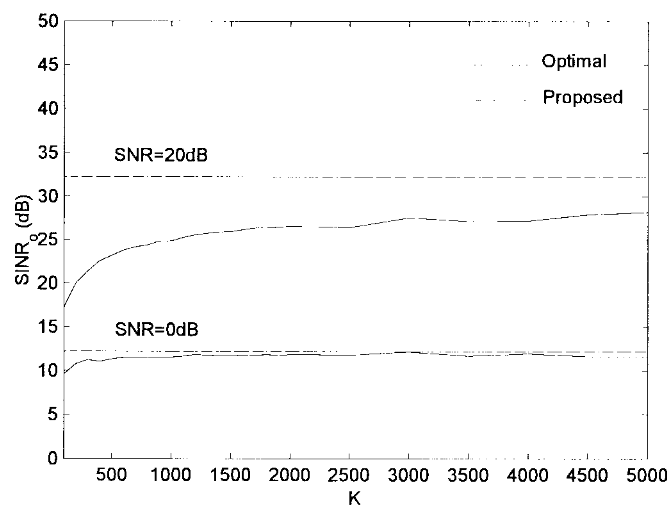

Fig. 8. Convergence behavior of proposed combiner with SNR $= 0$ and 20 dB.

In particular, the desired beam produces a null at $\theta \approx -10^\circ$ in an attempt to suppress CCI-2.

Finally, to investigate the convergence behavior of the combiner, we used different sample size K for computing $\hat{\boldsymbol{R}}_{xx}$, and plot the resulting output SINR in Fig. 8 for SNR $= 0$ and 20 dB. As expected, the output SINR increases as the sample size increases, approaching $\mathrm{SINR}_{\mathrm{opt}}$ for both

SNR levels. However, a result similar to that observed in the first simulation is that the combiner performs relatively poorer at high SNR. This is again due to the use of SB transformation with a finite sample size. It should be mentioned that the degradation at high SNR does not raise practical problems since the combiner can be switched to the decision directed mode as long as the CCI is sufficiently suppressed. That is, as an initial acquisition device, the proposed combiner is not required to perform a very precise cancellation of the CCI.

VI. Conclusion

An adaptive beam diversity combiner for combating multipath fading and cochannel interference is proposed for sectorized signal reception. The development of the combiner involved a two-stage procedure: formation of a bank of LCMV beams encompassing a prescribed angular sector, and combining of these adaptive beams into a single receiver with the maximum SNR gain. In order to avoid signal cancellation as usually incurred with coherent multipaths, a signal-blocking transformation was incorporated in the stage of beamforming. Cascading the two stages, a beamformer results which constructively combines the multipath signals from inside the working sector, and eliminates strong out-of-sector cochannel interference. This greatly enhances the performance of the system. A scheme is also suggested for discriminating the desired signal from possible in-sector interference. Simulation results shows that the proposed diversity combiner exhibits robustness against variations in environmental parameters and a significant performance enhancement as compared to the conventional nonadaptive receivers.

References

[1] S. H. Lin, T. C. Lee, and M. F. Gardina, "Diversity protections for digital radio: Summary of ten-year experiments and studies," *IEEE Commun. Mag.*, vol. 26, pp. 51–64, Feb. 1988.

[2] Swedish Telecom Radio Laboratory, "Antenna pattern diversity test with a 250 kbits/s modem at 900 MHz," in *Proc. 8th European Conf. Electrotechnics*, 1988, pp. 306–309.

[3] D. Vergeres, P. Jordi, and A. Loembe, "Simultaneous error performance of antenna pattern diversity and vertical space diversity on a 64-QAM radio link," in *Proc. IEEE GLOBECOM*, 1990, pp. 817–821.

[4] L. C. Godara, "Applications of antenna arrays to mobile communications, part I: Performance improvement, feasibility, and system considerations," *Proc. IEEE*, vol. 85, pp. 1031–1060, July 1990.

[5] W. C. Y. Lee, *Mobile Communications Engineering*. New York: McGraw-Hill, 1982.

[6] B. Widrow, K. M. Duvall, R. P. Gooch, and W. C. Newman, "Signal cancellation phenomena in adaptive antennas: causes and cures," *IEEE Trans. Antennas Propagat.*, vol. 30, pp. 469–478, May 1982.

[7] B. D. Van Veen and K. M. Buckley, "Beamforming: A versatile approach to spatial filtering," *IEEE ASSP Mag.*, pp. 4–24, Apr. 1988.

[8] R. Price and J. P. E. Green, "A communication technique for multipath channels," *Proc. IRE*, vol. 46, pp. 555–570, Mar. 1958.

[9] J. H. Winters, J. S. Salz, and R. D. Gitlin, " The impact of antenna diversity on the capacity of wireless communication systems," *IEEE Trans. Commun.*, vol. 42, pp. 1740–1751, Feb./Mar./Apr. 1994.

[10] S. Haykin, *Adaptive Filter Theory*. Englewood Cliffs, NJ: Prentice-Hall, 1996.

[11] S. Anderson, M. Millnert, M. Viberg, and B. Wahlberg, "An adaptive array for mobile communication systems," *IEEE Trans. Veh. Technol.*, vol. 40, pp. 230-236, Feb. 1991.

[12] B. Sklar, "Rayleigh fading channels in mobile digital communication systems," *IEEE Commun. Mag.*, pp. 90–109, July 1997.

[13] D. G. Luenberger, *Optimization by Vector Space Methods*. New York: Wiley, 1969, ch. 4, pp. 84–86.

[14] M. C. Doğan and J. M. Mendel, "Cumulant-based blind optimum beamforming," *IEEE Trans. Aerosp. Electron. Syst.*, vol. 30, pp. 722–741, July 1994.

[15] S. Sakagami, S. Aoyama, K. Kuboi, S. Shirota, and A. Akeyama, "Vehicle position estimates by multibeam antennas in multipath environments," *IEEE Trans. Veh. Technol.*, vol. 41, pp. 63–67, Feb. 1992.

[16] B. G. Agee, S. V. Schell, and W. A. Gardner, "Spectral self-coherence restoral: A new approach to blind adaptive signal extraction antenna arrays," *Proc. IEEE*, vol. 78, pp. 753–767, Apr. 1990.

[17] A. J. Paulraj and C. B. Papadias, "Space-time processing for wireless communications," *IEEE Signal Processing Mag.*, pp. 49–83, Nov. 1997.

Ta-Sung Lee (S'88–M'89) was born in Taipei, Taiwan, R.O.C., on October 20, 1960. He received the B.S. degree from National Taiwan University in 1983, the M.S. degree from the University of Wisconsin, Madison, in 1987, and the Ph.D. degree from Purdue University, West Lafayette, IN, in 1989, all in electrical engineering.

From 1987 to 1989, he was a David Rose Graduate Research Fellow of National Chiao Tung University, Hsinchu, Taiwan, where he currently holds a position of Professor in the Department of Communication Engineering. His research interests include sensor array signal processing, adaptive equalization, and smart antennas for wireless communications.

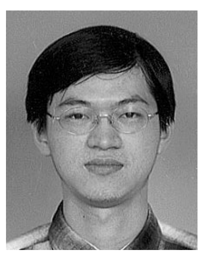

Zong Si Lee was born in Kaohsiung, Taiwan, R.O.C., on August 30, 1972. He received the B.S. degree in electrical engineering from National Cheng Kung University in 1995 and the M.S. degree in communication engineering from National Chiao Tung Univevrsity, Hsinchu, Taiwan, in 1997.

In 1998, he joined the Chung Shan Institute of Science and Technology (CSIST) as an Assistant Researcher. His current research interest is in intelligent vehicle highway systems.